Influence of the metal-to-ligand ratio on the formation of metal organic complexes†‡

Liliana Dobrzańska, Dewald J. Kleinhans and Leonard J. Barbour*

Received (in Durham, UK) 15th January 2008, Accepted 14th March 2008
First published as an Advance Article on the web 27th March 2008
DOI: 10.1039/b800720a

Three copper(II) salts with a chloride, bromide or nitrate counterions in combination with the ditopic ligand 1,3-bis(imidazol-1-ylmethyl)benzene (**L**) were used to study the influence of the metal to ligand molar ratio on the formation of the final product. Single-crystal X-ray analysis revealed structural diversity of the products formed, ranging from discrete species to extended 1D and 2D coordination polymers. Similar types of 1D chains were formed for all counterions.

Introduction

Structure prediction is still one of the most interesting and pressing aspects of the field of crystal engineering.[1] Indeed, many groups devote considerable effort to the elucidation of diverse factors that influence the process of crystallisation, and hence the resulting structure.[2] This requires a systematic approach since, in addition to the nature of the building blocks,[3] the structure adopted can also depend on the choice of solvent,[4] temperature[5] and the molar ratios of the molecular components.[6] Structure prediction is further complicated by the frequent occurrence of polymorphism, supramolecular isomerism and multicomponent crystals such as co-crystals or solvates.[7] Gaining insight into the role of any of the various structure-directing factors represents an important step towards driving the process of crystallisation in the desired direction.

Supramolecular isomerism[8] can be loosely described as the formation of multiple types of framework superstructure by a given set of (usually host) components, and with fixed stoichiometry. This phenomenon has not yet gained widespread recognition and, to date, only a few reports have described "proper" supramolecular isomers.[9] On the other hand, pseudo-supramolecular isomerism (implying different composition, usually due to the presence of solvent molecules) is far more common.[10]

The simultaneous formation of different polymorphs in the same crystal growth environment (*i.e.* "concomitant polymorphism")[11] is somewhat disconcerting with regard to our efforts to gain control over the process of crystallisation. It has been suggested[12] that the seemingly rare occurrence of concomitant polymorphism is mainly due to the general lack of effort aimed at searching for such phenomena. Indeed, this is a claim that we fully support.

As part of our ongoing studies of the different factors that influence the formation of metal complexes using imidazole derived ditopic ligands,[13] we decided to investigate the influence of the metal/ligand ratio in solution on the formation of the final solid product. We selected a ditopic ligand (**L** = 1,3-bis(imidazol-1-ylmethyl)benzene) with two imidazole rings occupying *meta* positions of a phenylene spacer group by means of methylene linkages (Scheme 1). The aim of this study was to use a conformationally flexible *exo*-bidentate ligand in order to explore its structural diversity when influenced by only one parameter (*i.e.* the metal/ligand molar ratio).

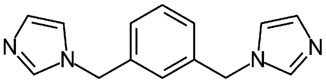

Scheme 1 1,3-Bis(imidazol-1-ylmethyl)benzene (**L**).

Results and discussion

Crystal growth

The crystals of the metal complexes presented here were prepared using metal to ligand (M : **L**) molar ratios of 1 : 4, 1 : 1 and 4 : 1 in methanol and the Cu(II) salts $CuCl_2{\cdot}2H_2O$, $CuBr_2$ and $Cu(NO_3)_2{\cdot}H_2O$ (see Table 1). Each solution was allowed to crystallise by slow evaporation over a period of several days to yield crystals suitable for single-crystal X-ray diffraction analysis.

Crystal structures

In all cases X-ray diffraction analysis proved to be unambiguous and no further analytical techniques were deemed necessary to verify the constituents of the crystals.

$[Cu_2L_2(\mu\text{-}Cl)_2Cl_2]$ (1). Complex **1** consists of a discrete dinuclear complex (Fig. 1) with each Cu ion in a distorted square-based pyramidal coordination environment.§ The vertices of the square consist of two imidazole nitrogen atoms (Cu–N = 1.971(3) and 1.981(3) Å) situated *trans* with respect to one another, a terminal chloride ion (Cu–Cl = 2.337(1) Å) and one of the two bridging chloride ions (Cu–Cl

---

Department of Chemistry, University of Stellenbosch, Matieland, 7602, South Africa. E-mail: ljb@sun.ac.za; Fax: +27 21-808-3849; Tel: +27 21-808-3335

† Dedicated to Professor Jerry Atwood on the occasion of his 65th birthday.

‡ CCDC reference numbers 681408–681415. For crystallographic data in CIF or other electronic format see DOI: 10.1039/b800720a

Table 1 M : **L** molar ratios used for the formation of **1**–**8** together with connectivity changes

Ratio M : **L**	$CuCl_2·2H_2O$	$CuBr_2$	$Cu(NO_3)_2·H_2O$
1 : 4	Blue prism (**2**) One-dimensional strand	Blue prism (**3**) One-dimensional strand	Violet block (**6**) One-dimensional strand Blue prism (**7**) One-dimensional strand
1 : 1	Green block (**1**) Discrete dinuclear complex	Blue prism (**3**) One-dimensional strand	Violet prism (**5**) 2D layers Violet block (**6**) One-dimensional strand
4 : 1	Green block (**1**) Discrete dinuclear complex	Green block (**4**) Discrete dinuclear complex	Blue plate (**8**) One-dimensional strand

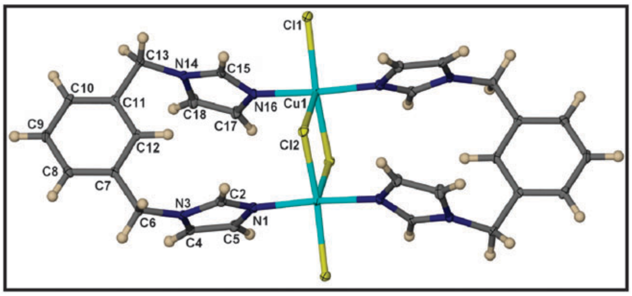

Fig. 1 Atomic displacement (50% probability) plot showing the molecular structure of complex **1**. Unlabeled atoms are related to labelled atoms by the symmetry operation −*x*, 2 − *y*, 1 − *z*.

= 2.339(1) Å). The apex of the pyramid consists of the remaining bridging chloride ion (2.698(1) Å) and the complex is situated on an inversion centre. The conformation of the *exo*-bidentate ligand **L** is approximately C-shaped such that it is able to coordinate simultaneously to both Cu ions which are separated by a distance of 3.555(1) Å. The complexes pack in the well-known herringbone arrangement as shown in Fig. 2.

($[CuL_2Cl_2]·2CH_3OH)_\infty$ (2). Complex **2** forms an infinite one-dimensional strand running parallel to [001] (see Fig. 3). Each metal centre is linked to an adjacent centre by means of two ligands **L**. Each copper ion is in an octahedral coordination environment and coordinates to four symmetry-related imidazole groups (Cu–N = 2.026(2) Å) that occupy the vertices of an almost ideal square plane (∠N–Cu–N = 90.46(10)° and 89.54(10)°). The apical positions of the octahedra are occupied by chloride ions (Cu–Cl = 2.832(1) Å) and the Cu–Cl bond forms an angle of 93.84° with respect to the square plane occupied by the imidazole nitrogen atoms. Furthermore, methanol solvent molecules are present in the structure and form O–H···Cl hydrogen bonds (O···Cl = 3.067(3) Å) to the ligated chloride ions.

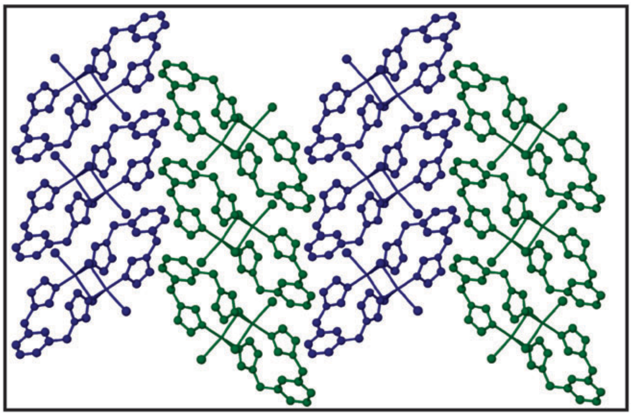

Fig. 2 Ball-and-stick plot showing the packing arrangement of **1** as viewed along [100]. Hydrogen atoms have been omitted for clarity and adjacent columns of the herringbone pattern are coloured green and blue to distinguish them from one another.

($[CuL_2(H_2O)_2]Br_2)_\infty$ (3). Complex **3** forms a 1D chain similar to that of **2** in that each metal centre in the chain is linked to an adjacent metal centre by means of two ligands **L** (Cu–N = 2.031(4) and 2.009(4) Å) which are situated on the square plane of an octahedral coordination environment (Fig. 4). However, the apical positions of the octahedra in **3** are occupied by water molecules (Cu–O = 2.498(4) Å) which are in turn hydrogen bonded to non-coordinated bromide ions (O···Br = 3.431(4) Å). By virtue of these hydrogen bonds and inversion symmetry, adjacent 1D strands are connected to one another to form 2D layers parallel to (101) as shown in Fig. 5.

$[Cu_2L_2(\mu\text{-}Br)_2Br_2]$ (4). The molecular structure of **4** is similar to that of **1** (see Table 2). Indeed, the unit cell parameters and space group are sufficiently similar that **1** and **4** can be considered to be isostructural (in a non-rigorous sense). The unique Cu–N distances are 1.970(3) and 1.969(3) Å and the Cu–Br distances in the square plane (terminal and bridging bromide ions) are 2.491(1) and 2.480(1) Å, respectively. The apical μ-Br is situated at a distance of 2.798(1) Å from the metal centre.

$[CuL_2(NO_3)_2]_\infty$ (5). The structure of **5** consists of 2D layers parallel to ($10\bar{2}$) as shown in Fig. 6. Each metal centre is in an octahedral coordination environment: imidazole groups are situated at the vertices of the square plane (unique Cu–N =

---

§ The coordination spheres given as square-based pyramids are in agreement with the geometric parameter τ formulated by Addison *et al.*[20] as an index of the degree of trigonality, which is close to 0 in both **1** and **8** but shows larger distortion in **1**. The values are as follows: 0.080 for **1** (N1^i–Cu1–N16 = 171.06(12), Cl1–Cu1–Cl2^i = 166.24(4); (i) −*x*, −*y* + 2, −*z* + 1) and 0.015 for **8** (O22–Cu1–O26 = 173.87(12), N1–Cu1–N16^i = 172.96(15); (i) *x* + 1/2, −*y* + 1/2, *z* − 1/2). The same parameter for **4** is 0.066 (N1^i–Cu1–N16 = 170.89(11), Br1–Cu1–Br2^i = 166.91(2); (i) −*x* + 1, −*y* + 1, −*z* + 1).

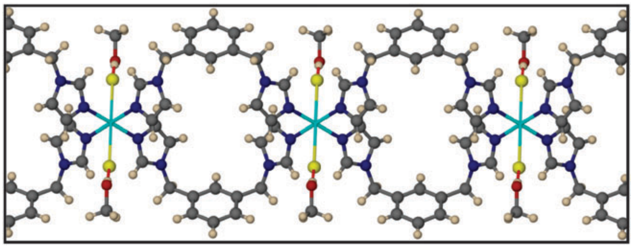

Fig. 3 Ball-and-stick plot showing the 1D chain formed by **2**. Colours: carbon, grey; hydrogen, white; nitrogen, dark blue; chloride, yellow; copper, light blue; oxygen, red.

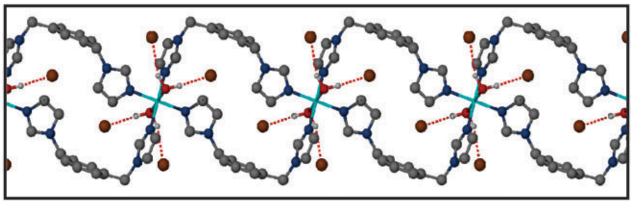

Fig. 4 Ball-and-stick plot showing the 1D chain formed by **3**. Bromide ions are coloured brown and hydrogen bonds are shown as dotted red lines.

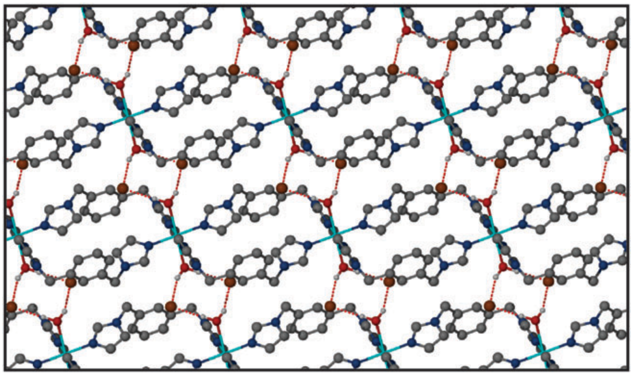

Fig. 5 Packing arrangement of **3** to form 2D layers parallel to [101].

2.021(2), 2.007(2) Å) and the apical positions are occupied by monodentate nitrate ions (Cu–O = 2.449(4) Å). Each ligand **L** bridges two Cu ions and assumes an approximate L-shaped conformation. The 2D layer consists of fused 48-membered rings each consisting of four Cu centres and four bridging ligands.

$[\mathrm{CuL_2(NO_3)_2}]_\infty$ (6). Complex **6** forms 1D strands in a fashion similar to those of **2** and **3**. Each metal centre is linked to its neighbour by means of two bridging ligands **L**, and is in an octahedral coordination environment (Fig. 7). The square plane is occupied by four imidazole groups (Cu–N = 1.994(3) and 1.995(3) Å), while the apical positions are occupied by monodentate nitrate anions (Cu–O = 2.647(4) Å).

Both **5** and **6** were isolated from the same solution consisting of a 1 : 1 molar ratio of Cu : **L** and both structures have the same chemical composition of $\mathrm{C_{28}H_{28}CuN_{10}O_6}$.

$([\mathrm{CuL_2(CH_3OH)_2}][\mathrm{CuL_2(H_2O)_2}](\mathrm{NO_3})_4\cdot 2\mathrm{H_2O})_\infty$ (7). The asymmetric unit of **7** consists of two metal ions, two ligands **L**, two nitrate ions, two water molecules and one molecule of methanol. The structure contains two unique 1D strands, both running parallel to [100] (see Fig. 8). Both strands consist of metal centres doubly linked to one another by means of ligand **L** as observed in **2**, **3** and **6**. However, the apical positions of the octahedra in one strand are occupied by water molecules while those of the other strand are occupied by methanol molecules. One of these water molecules is hydrogen bonded to a nitrate anion (O···O = 2.831(12) Å) and to non-coordinated water molecule (O···O = 2.690(2) Å). The latter in turn donates a hydrogen bond (O···O = 2.820(2) Å) to another nitrate anion. A different oxygen atom of the latter is hydrogen bonded (O···O = 2.826(9) Å) to a methanol oxygen atom

Table 2 Selected bond distances (Å) and angles (°) for complexes **1** and **4**

Compound **1**			
Cu(1)–N(1)^{i}	1.971(3)	Cu(1)–Cl(2)	2.698(1)
Cu(1)–N(16)	1.981(3)	Cu(1)–Cl(1)	2.337(1)
Cu(1)–Cl(2)^{i}	2.339(1)		
N(1)^{i}–Cu(1)–N(16)	171.06(12)	N(1)^{i}–Cu(1)–Cl(2)	92.81(9)
N(1)^{i}–Cu(1)–Cl(1)	88.41(9)	N(16)–Cu(1)–Cl(2)	96.11(9)
N(16)–Cu(1)–Cl(1)	88.94(9)	Cl(1)–Cu(1)–Cl(2)	103.17(3)
N(1)^{i}–Cu(1)–Cl(2)^{i}	89.21(9)	Cl(2)^{i}–Cu(1)–Cl(2)	90.48(3)
N(16)–Cu(1)–Cl(2)^{i}	91.35(9)	Cu(1)^{i}–Cu(2)–Cl(1)	89.52(3)
Cl(1)–Cu(1)–Cl(2)	166.24(4)		
Compound **4**			
Cu(1)–N(1)^{i}	1.970(3)	Cu(1)–Br(2)	2.798(1)
Cu(1)–N(16)	1.969(3)	Cu(1)–Br(1)	2.491(1)
Cu(1)–Br(2)^{i}	2.480(1)		
N(1)^{i}–Cu(1)–N(16)	170.89(11)	N(1)^{i}–Cu(1)–Br(2)	93.79(9)
N(1)^{i}–Cu(1)–Br(1)	88.01(8)	N(16)–Cu(1)–Br(2)	95.25(9)
N(16)–Cu(1)–Br(1)	89.20(9)	Br(1)–Cu(1)–Br(2)	101.21(3)
N(1)^{i}–Cu(1)–Br(2)^{i}	89.40(8)	Br(2)^{i}–Cu(1)–Br(2)	91.76(3)
N(16)–Cu(1)–Br(2)^{i}	91.36(9)	Cu(1)^{i}–Br(2)–Cu(1)	88.24(3)
Br(1)–Cu(1)–Br(2)^{i}	166.91(2)		

Symmetry transformations used to generate equivalent positions: **1** (i) $-x, -y + 2, -z + 1$; **4** (i) $-x + 1, -y + 1, -z + 1$.

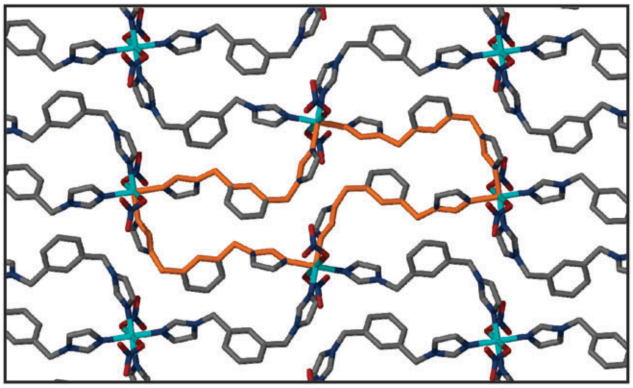

Fig. 6 Capped-stick representation of the 2D layers formed by **5**. Hydrogen atoms have been omitted for clarity and a selected 48-membered ring is indicated by orange bonds.

which is also coordinated to the Cu ion of an adjacent strand. It is interesting that crystals of both **6** and **7** were isolated from a solution containing a M : **L** ratio of 1 : 4.

$[CuL(H_2O)(NO_3)_2]_\infty$ (8). In **8** the Cu ions are in a square-based pyramidal coordination environment.§ The vertices of the square base are occupied by two ligands **L** situated *trans* to one another (Cu–N = 1.966(4) and 1.959(3) Å), and by two *trans*-coordinated NO_3 anions (Cu–O = 2.041(3) and 2.033(3) Å). The apical position is occupied by a water molecule (Cu–O = 2.269(3) Å). A 1D strand running parallel to $[10\bar{1}]$ is formed (Fig. 9) in which neighbouring Cu ions are linked to one another by means of a single bridging ligand **L**. The ligated water molecules and nitrate ions cooperate in the formation of hydrogen bonds that link strands to one another along [010] and result in 2D layers (see ESI‡ for details of hydrogen bonding parameters) (Fig. 10).

Effect of molar ratios

It is interesting to compare the effect of the solution M : **L** molar ratios for the $CuCl_2{\cdot}2H_2O$ and $CuBr_2$ salts with regard to the resulting M : **L** ratios in the solid state. In both cases, when the relative M : **L** ratio is high (*i.e.* 4 : 1), a dinuclear complex with an overall M : **L** ratio of 1 : 1 is formed. Indeed, these complexes (**1** and **4**) are structural analogues of one another and also pack in the same manner. When the M : **L** ratio is low (*i.e.* 1 : 4), an infinite 1D strand with M : **L** = 1 : 2 is formed in both cases. The most significant difference between the structures of **2** and **3** is the nature of the apical coordination sites of the octahedra. In **2**, these sites are occupied by chloride ions which are hydrogen bonded to non-coordinated methanol molecules. In **3**, the apical sites are occupied by water molecules which hydrogen bond to non-coordinated bromide ions. Although the formation of **1** to **4** from either high or low M : **L** molar ratios as described above is somewhat intuitive, it is less obvious why 1 : 1 solutions might produce vastly different results for $CuCl_2{\cdot}2H_2O$ and $CuBr_2$. In the former, the solution 1 : 1 ratio is reflected in the resulting solid state complex **1**. However, in the case of the latter, the 1 : 1 solution yields the same solid state structure as the 1 : 4 solution (*i.e.* **3** with M : **L** = 1 : 2). Perhaps the simple explanation is that under the conditions of crystallisation, Cu binds more readily to Cl than to H_2O, but more readily to H_2O than to Br.

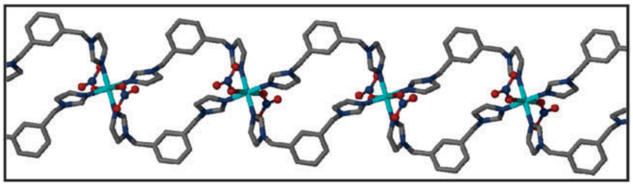

Fig. 7 Capped-stick representation of the 1D strands formed by **6**. Hydrogen atoms have been omitted for clarity and nitrate ions are shown in the ball-and-stick metaphor.

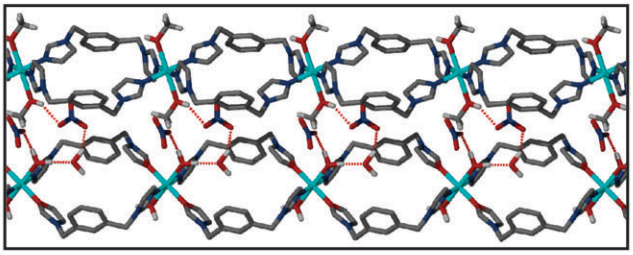

Fig. 8 Capped-stick representation of the 1D strands formed in **7**. Ligand hydrogen atoms have been omitted for clarity and hydrogen bonds are indicated by dotted red lines.

It is more revealing to compare the four structures obtained using $Cu(NO_3)_2{\cdot}H_2O$ (**5**–**8**) with one another than with those obtained from $CuCl_2{\cdot}2H_2O$ and $CuBr_2$ (**1**–**4**). Only one structure (*i.e.* **8**) was observed to crystallise from the solution with M : **L** = 4 : 1 and, as may be expected, this structure has the highest M : **L** ratio (*i.e.* 1 : 1). In contrast, structures **5** to **7** all have a M : **L** ratio of 1 : 2. Structure **6** forms from both the 1 : 4 and 1 : 1 solutions and is reminiscent of the structures of **2** and **3**. This perhaps indicates that this structure type is preferred for this particular ligand when the M : **L** ratio is less than or equal to unity. Of significant interest is that the 1 : 4 and 1 : 1 solutions both yielded two different crystal forms (see phase identification in the ESI‡): form **5** crystallised concomitantly with form **6** from the 1 : 1 solution (estimation of *ca.* 6 vol% of **5** and 94 vol% of **6** in the resulting mixture—see ESI‡), whereas a few blue crystals of **7** appeared after a few weeks among violet crystals of form **6** from the 1 : 4 solution, probably due to the influence of water molecules. Form **6** shares similarities with both **5** and **7**. The coordination environments about the metal centres in both **5** and **6** consist of octahedra with ligands **L** at the corners of a square plane, and nitrates at the apical positions. The major difference is that **5** forms a 2D network while **6** forms a 1D chain. Forms **5** and **7** both form 1D chains with each metal centre linked to its neighbour by means of two ligands **L**. In both structures, **L** occupies the corners of a square plane of the octahedra but, whereas the apical positions

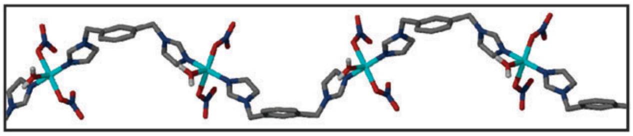

Fig. 9 Capped-stick representation of the 1D strands formed in **8**. Ligand hydrogen atoms have been omitted for clarity.

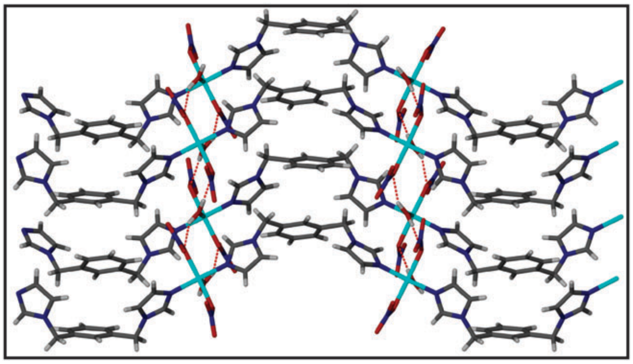

Fig. 10 Capped-stick representation of the formation of 2D layers in **8** by hydrogen bonding, with hydrogen bonds indicated as dotted red lines.

of **6** are occupied by nitrate anions, these positions are occupied by methanol molecules in **7**.

Nomenclature

A comparison of the structures of **5** and **6** raises interesting questions about the nomenclature of crystal forms.[14] Since **5** and **6** have the same structural formula (*i.e.* $[Cu_2\mathbf{L}(NO_3)_2]_\infty$), it is tempting to consider these forms to be concomitant polymorphs[11] of one another. Polymorphism can loosely be described as different arrangements of the same structural component(s). As suggested by Desiraju,[7a] the definition of a structural unit can be subjective: when one considers interactions such as hydrogen bonds, coordination bonds and covalent bonds, the question of whether **5** and **6** are polymorphs of one another depends on where one draws the line with regard to the formation of atomic or molecular networks. Most solid-state chemists would probably agree that polymorphs could have different hydrogen bonding patterns, but not different covalent connectivity. However, does one classify coordination bonds together with hydrogen bonds or with covalent bonds in this context? We believe that the latter is more appropriate and that a good analogy is provided by a comparison of the structures of cisplatin and transplatin. These compounds are simply structural isomers that can be considered as distinctly different such that their structures would not be considered to be polymorphs.

Conclusions

We have conducted a systematic study to show that the metal-to-ligand molar ratio in solution plays an important role with regard to the structures of the resulting crystals. In general, the use of excess ligand leads to the formation of extended one- or two-dimensional polymeric systems. In one case, we observed the concomitant crystallisation of different crystal forms from the same solution, and we believe that this phenomenon is probably more common in coordination chemistry than it is generally thought to be. In many cases there may be no obvious difference in crystal morphology or the colour of concomitant forms, and this fascinating phenomenon might thus go unnoticed without the routine (albeit tedious) application of X-ray powder diffraction to screen the bulk crystalline material.

Experimental

Reagents and materials

All commercially available chemicals were of reagent grade and were used without further purification. The ditopic ligand 1,3-bis(imidazol-1-ylmethyl)benzene (**L**), was synthesised by the S_N2 reaction of imidazole with α,α′-dibromo-*m*-xylene. The metal complexes were obtained in methanol (40 ml) by using a 1 : 1, 1 : 4 and 4 : 1 ratio of metal salt to ligand, respectively. The phase composition of the crystals that deposited, was verified using X-ray powder diffraction of the bulk solid material in each case.

X-Ray crystallography

Single-crystal X-ray diffraction data were collected on a Bruker SMART APEX[15] diffractometer equipped with graphite-monochromated Mo-Kα radiation (λ = 0.71073 Å). The crystals were coated with Paratone-N oil and mounted on a glass fiber. Data collection was carried out at 100(2) K to minimise solvent loss, possible structural disorder and thermal motion effects. Cell refinement and data reduction were performed using the program SAINT[16] and all empirical absorption corrections were performed using SADABS.[17] Each structure was solved by direct methods using SHELXS-97[17] and refined by full-matrix least-squares methods based on F^2 using SHELXL-97[17] and using the graphics interface program X-Seed.[18] The programs X-Seed and POV-Ray[19] were both used to prepare molecular graphics images. All non-hydrogen atoms were refined anisotropically. All hydrogen atoms, except the O–H hydrogen atoms obtained from a difference Fourier map and refined independently, were positioned geometrically with C–H = 0.95 (aromatic), 0.98 (methyl) and 0.99 Å (methylene) and refined as riding on their parent atoms, with U_{iso}(H) = 1.2 U_{eq} (C) and 1.5 U_{eq} (methyl C). X-ray powder diffraction (XRPD) intensities for the products of different M : **L** molar ratios with nitrate counterion (ESI‡) were measured at 293 K on a Bruker D8 Advance Diffractometer (Cu-Kα, λ = 1.54056 Å).

Crystal data for 1

$C_{28}H_{28}Cl_4Cu_2N_8$, M = 745.46, green block, 0.34 × 0.25 × 0.16 mm^3, monoclinic, space group $P2_1/c$ (no. 14), a = 9.0726(13), b = 7.3982(11), c = 22.319(3) Å, β = 98.604(2)°, V = 1481.2(4) Å^3, Z = 2, D_c = 1.671 g cm^{-3}, F_{000} = 756, Mo-Kα radiation, λ = 0.71073 Å, T = 100(2) K, $2\theta_{max}$ = 56.6°, 8203 reflections collected, 3413 unique (R_{int} = 0.0408). Final *GooF* = 1.114, $R1$ = 0.0532, $wR2$ = 0.1098, R indices based on 2835 reflections with $I > 2\sigma(I)$ (refinement on F^2), 190 parameters, 0 restraints. Lp and absorption corrections applied, μ = 1.832 mm^{-1}.

Crystal data for 2

$C_{30}H_{36}Cl_2CuN_8O_2$, M = 675.11, blue prism, 0.24 × 0.11 × 0.09 mm^3, orthorhombic, space group $Pnnm$ (no. 58), a = 17.992(3), b = 7.6710(12), c = 11.3090(18) Å, V = 1560.8(4)

Å^3, $Z = 2$, $D_c = 1.436$ g cm^{-3}, $F_{000} = 702$, Mo-Kα radiation, $\lambda = 0.71073$ Å, $T = 100(2)$ K, $2\theta_{\max} = 56.5°$, 9262 reflections collected, 1949 unique ($R_{\text{int}} = 0.0514$). Final $GooF = 1.123$, $R1 = 0.0453$, $wR2 = 0.0944$, R indices based on 1605 reflections with $I > 2\sigma(I)$ (refinement on F^2), 111 parameters, 0 restraints. Lp and absorption corrections applied, $\mu = 0.913$ mm^{-1}.

Crystal data for 3

$C_{28}H_{32}Br_2CuN_8O_2$, $M = 735.98$, blue prism, $0.18 \times 0.15 \times 0.08$ mm^3, triclinic, space group $P\bar{1}$ (no. 2), $a = 8.683(2)$, $b = 8.762(2)$, $c = 10.844(2)$ Å, $\alpha = 75.252(4)$, $\beta = 67.904(4)$, $\gamma = 80.906(4)°$, $V = 737.4(3)$ Å^3, $Z = 1$, $D_c = 1.657$ g cm^{-3}, $F_{000} = 371$, Mo-Kα radiation, $\lambda = 0.71073$ Å, $T = 100(2)$ K, $2\theta_{\max} = 56.5°$, 8492 reflections collected, 3382 unique ($R_{\text{int}} = 0.0632$). Final $GooF = 1.020$, $R1 = 0.0542$, $wR2 = 0.0970$, R indices based on 2466 reflections with $I > 2\sigma(I)$ (refinement on F^2), 195 parameters, 3 restraints. Lp and absorption corrections applied, $\mu = 3.491$ mm^{-1}.

Crystal data for 4

$C_{28}H_{28}Br_4Cu_2N_8$, $M = 923.28$, green block, $0.28 \times 0.24 \times 0.21$ mm^3, monoclinic, space group $P2_1/c$ (no. 14), $a = 9.264(5)$, $b = 7.469(4)$, $c = 22.621(11)$ Å, $\beta = 98.926(9)°$, $V = 1546.3(14)$ Å^3, $Z = 2$, $D_c = 1.983$ g cm^{-3}, $F_{000} = 900$, Mo-Kα radiation, $\lambda = 0.71073$ Å, $T = 100(2)$ K, $2\theta_{\max} = 56.9°$, 9476 reflections collected, 3639 unique ($R_{\text{int}} = 0.0428$). Final $GooF = 1.009$, $R1 = 0.0344$, $wR2 = 0.0777$, R indices based on 3051 reflections with $I > 2\sigma(I)$ (refinement on F^2), 190 parameters, 0 restraints. Lp and absorption corrections applied, $\mu = 6.578$ mm^{-1}.

Crystal data for 5

$C_{28}H_{28}CuN_{10}O_6$, $M = 664.14$, violet prism, $0.28 \times 0.20 \times 0.11$ mm^3, monoclinic, space group $P2_1/c$ (no. 14), $a = 11.336(5)$, $b = 9.369(4)$, $c = 13.865(6)$ Å, $\beta = 103.089(8)°$, $V = 1434.3(11)$ Å^3, $Z = 2$, $D_c = 1.538$ g cm^{-3}, $F_{000} = 686$, Mo-Kα radiation, $\lambda = 0.71073$ Å, $T = 100(2)$ K, $2\theta_{\max} = 56.8°$, 8758 reflections collected, 3332 unique ($R_{\text{int}} = 0.0501$). Final $GooF = 1.061$, $R1 = 0.0536$, $wR2 = 0.1089$, R indices based on 2671 reflections with $I > 2\sigma(I)$ (refinement on F^2), 205 parameters, 0 restraints. Lp and absorption corrections applied, $\mu = 0.824$ mm^{-1}.

Crystal data for 6

$C_{28}H_{28}CuN_{10}O_6$, $M = 664.14$, violet block, $0.18 \times 0.15 \times 0.13$ mm^3, monoclinic, space group $C2/c$ (no. 15), $a = 14.821(6)$, $b = 8.908(4)$, $c = 21.365(9)$ Å, $\beta = 93.632(8)°$, $V = 2815(2)$ Å^3, $Z = 4$, $D_c = 1.567$ g cm^{-3}, $F_{000} = 1372$, Mo-Kα radiation, $\lambda = 0.71073$ Å, $T = 100(2)$ K, $2\theta_{\max} = 56.5°$, 8521 reflections collected, 3247 unique ($R_{\text{int}} = 0.0489$). Final $GooF = 1.177$, $R1 = 0.0785$, $wR2 = 0.1485$, R indices based on 2716 reflections with $I > 2\sigma(I)$ (refinement on F^2), 205 parameters, 0 restraints. Lp and absorption corrections applied, $\mu = 0.840$ mm^{-1}.

Crystal data for 7

$C_{58}H_{70}Cu_2N_{18}O_{19}$, $M = 1450.40$, blue prism, $0.24 \times 0.18 \times 0.13$ mm^3, triclinic, space group $P\bar{1}$ (no. 2), $a = 8.7647(14)$, $b = 10.8794(17)$, $c = 16.984(3)$ Å, $\alpha = 89.797(3)$, $\beta = 89.368(3)$, $\gamma = 84.603(3)°$, $V = 1612.2(4)$ Å^3, $Z = 1$, $D_c = 1.494$ g cm^{-3}, $F_{000} = 754$, Mo-Kα radiation, $\lambda = 0.71073$ Å, $T = 100(2)$ K, $2\theta_{\max} = 56.7°$, 18 918 reflections collected, 7524 unique ($R_{\text{int}} = 0.0805$). Final $GooF = 1.012$, $R1 = 0.0811$, $wR2 = 0.1743$, R indices based on 4628 reflections with $I > 2\sigma(I)$ (refinement on F^2), 463 parameters, 13 restraints. Lp and absorption corrections applied, $\mu = 0.747$ mm^{-1}.

Crystal data for 8

$C_{14}H_{16}CuN_6O_7$, $M = 443.87$, blue plate, $0.16 \times 0.14 \times 0.03$ mm^3, monoclinic, space group $P2_1/n$ (no. 14), $a = 9.841(4)$, $b = 8.311(3)$, $c = 21.919(8)$ Å, $\beta = 101.047(7)°$, $V = 1759.4(11)$ Å^3, $Z = 4$, $D_c = 1.676$ g cm^{-3}, $F_{000} = 908$, Mo-Kα radiation, $\lambda = 0.71073$ Å, $T = 100(2)$ K, $2\theta_{\max} = 56.6°$, 10 495 reflections collected, 4040 unique ($R_{\text{int}} = 0.0655$). Final $GooF = 1.034$, $R1 = 0.0673$, $wR2 = 0.1313$, R indices based on 2712 reflections with $I > 2\sigma(I)$ (refinement on F^2), 261 parameters, 3 restraints. Lp and absorption corrections applied, $\mu = 1.295$ mm^{-1}.

Acknowledgements

We thank the National Research Foundation and the South African Research Chair Initiative for support of this work.

References

1 (*a*) J. Maddox, *Nature*, 1988, **335**, 201; (*b*) A. Gavezzotti, *Acc. Chem. Res.*, 1994, **27**, 309; (*c*) J. Dunitz, *Chem. Commun.*, 2003, **5**, 545.
2 (*a*) M. J. Zaworotko, *Cryst. Growth Des.*, 2007, **7**, 4; (*b*) J.-P. Zhang and X.-M. Chen, *Chem. Commun.*, 2006, 1689; (*c*) J. D. Wuest, *Chem. Commun.*, 2005, 5830; (*d*) O. M. Yaghi, M. O'Keefe, N. W. Ockwig, H. K. Chae, M. Eddaoudi and J. Kim, *Nature*, 2003, **423**, 705; (*e*) A. J. Blake, N. R. Champness, P. Hubberstey, W. S. Li, M. A. Withersby and M. Schröder, *Coord. Chem. Rev.*, 1999, **183**, 117; (*f*) D. Braga, F. Grepioni and G. R. Desiraju, *Chem. Rev.*, 1998, **98**, 1375; (*g*) *Frontiers in Crystal Engineering*, ed. E. R. T. Tiekink and J. J. Vittal, Wiley, Chichester, 2006.
3 (*a*) L. Brammer, *Chem. Soc. Rev.*, 2004, **33**, 476; (*b*) C. B. Aakeroy, *Acta Crystallogr., Sect. B*, 1997, **53**, 569.
4 (*a*) N. Blagden, R. J. Davey, H. F. Lieberman, L. Williams, R. Payne, R. Roberts, R. Rowe and R. Docherty, *J. Chem. Soc., Faraday Trans.*, 1998, **94**, 1035; (*b*) S. Khoshkhoo and J. Anwar, *J. Phys. D: Appl. Phys.*, 1993, **26**, 890; (*c*) L. Dobrzańska, G. O. Lloyd and L. J. Barbour, *New J. Chem.*, 2007, **31**, 669.
5 P. Raiteri, R. Marton and M. Parrinello, *Angew. Chem., Int. Ed.*, 2005, **44**, 3769.
6 (*a*) J. Y. Lu, B. R. Cabrera, R.-J. Wang and J. Li, *Inorg. Chem.*, 1999, **38**, 4608; (*b*) R. P. Feazell, C. E. Carson and K. K. Klausmeyer, *Inorg. Chem.*, 2006, **45**, 2627; (*c*) M. Oh, C. L. Stern and C. A. Mirkin, *Inorg. Chem.*, 2005, **44**, 2647; (*d*) G. W. Orr, L. J. Barbour and J. L. Atwood, *Science*, 1999, **285**, 1049.
7 (*a*) G. R. Desiraju, *Nat. Mater.*, 2002, **1**, 77; (*b*) A. J. C. Cabeza, G. M. Day, W. D. S. Motherwell and W. Jones, *J. Am. Chem. Soc.*, 2006, **128**, 14466; (*c*) J. W. Chew, S. N. Black, P. S. Chow, R. B. H. Tanc and K. J. Carpenter, *CrystEngComm*, 2007, **9**, 128.
8 B. Moulton and M. J. Zaworotko, *Chem. Rev.*, 2001, **101**, 1629.
9 (*a*) D. J. Ring, M. C. Aragoni, N. R. Champness and C. Wilson, *CrystEngComm*, 2005, **7**, 621; (*b*) S. Lipstman, S. Muniappan and I. Goldberg, *Acta Crystallogr., Sect. C*, 2007, **63**, o371; (*c*) B. Rather, B. Moulton, R. D. B. Walsh and M. J. Zaworotko, *Chem. Commun.*, 2002, 694.
10 (*a*) X. Yang, J. D. Ranford and J. J. Vittal, *Cryst. Growth Des.*, 2004, **4**, 781; (*b*) W. L. Leong and J. J. Vittal, *Cryst. Growth Des.*, 2007, **7**, 2112.

11 J. Bernstein, R. E. Davis, L. Shimoni and N.-L. Chang, *Angew. Chem., Int. Ed. Engl.*, 1995, **34**, 1555.

12 K. F. Bowes, C. Glidwell, J. N. Low, J. M. S. Skakle and J. L. Wardell, *Acta Crystallogr., Sect. C*, 2003, **59**, o1.

13 (*a*) L. Dobrzańska, G. O. Lloyd, H. G. Raubenheimer and L. J. Barbour, *J. Am. Chem. Soc.*, 2005, **127**, 13134; (*b*) L. Dobrzańska, G. O. Lloyd, H. G. Raubenheimer and L. J. Barbour, *J. Am. Chem. Soc.*, 2006, **128**, 698; (*c*) L. Dobrzańska, G. O. Lloyd, C. Esterhuysen and L. J. Barbour, *Angew. Chem., Int. Ed.*, 2006, **45**, 5856; (*d*) L. Dobrzańska, G. O. Lloyd, T. Jacobs, I. Rootman, C. L. Oliver, M. W. Bredenkamp and L. J. Barbour, *J. Mol. Struct.*, 2006, **796**, 107.

14 G. R. Desiraju, *Cryst. Growth Des.*, 2008, **8**, 3.

15 SMART Version 5.625, Bruker AXS Inc., Madison, WI, USA, 2001.

16 SAINT Version 6.36a, Bruker AXS Inc., Madison, WI, USA, 2002.

17 G. M. Sheldrick, SHELXS-97, SHELXL-97 and SADABS Version 2.05, University of Göttingen, Germany, 1997.

18 (*a*) L. J. Barbour, *J. Supramol. Chem.*, 2001, **1**, 189; (*b*) J. L. Atwood and L. J. Barbour, *Cryst. Growth Des.*, 2003, **3**, 3.

19 http://www.povray.org.

20 A. W. Addison, T. Nageswara Rao, J. Reedijk, J. van Rijn and G. C. Verschoor, *J. Chem. Soc., Dalton Trans.*, 1984, 1349.